Precipitation changes in the Mediterranean basin during the Holocene from terrestrial and marine pollen records: A model/data comparison

Odile Peyron[1], Nathalie Combourieu-Nebout[2], David Brayshaw[3], Simon Goring[4], Valérie Andrieu-Ponel[5], Stéphanie Desprat[6,7], Will Fletcher[8], Belinda Gambin[9], Chryssanthi Ioakim[10], Sébastien Joannin[1], Ulrich Kotthoff[11], Katerina Kouli[12], Vincent Montade[1], Jörg Pross[13], Laura Sadori[14], Michel Magny[15]

[1] Institut des Sciences de l'Evolution (ISEM), Université de Montpellier, France

[2] UMR 7194 MNHN, Institut de Paléontologie Humaine 1, Paris, France

[3] University of Reading, Department of Meteorology, United Kingdom

[4] Department of Geography, Univ. of Wisconsin-Madison, Wisconsin, USA

[5] Institut Méditerranéen de Biodiversité et d'Ecologie marine et continentale (IMBE), Aix Marseille Université, Aix-en-Provence, France

[6] EPHE, PSL Research University, Laboratoire Paléoclimatologie et Paléoenvironnements Marins, Pessac, France

[7] Univ. Bordeaux, EPOC UMR 5805, Pessac, France

[8] Geography, School of Environment, Education and Development, University of Manchester, United Kingdom

[9] Institute of Earth Systems, University of Malta, Malta

[10] Institute of Geology and Mineral Exploration, Athens, Greece

[11] Center for Natural History and Institute of Geology, Hamburg University, Hamburg, Germany

[12] Department of Geology and Geoenvironment, National and Kapodistrian University of Athens, Greece

[13] Paleoenvironmental Dynamics Group, Institute of Earth Sciences, Heidelberg University, Germany

[14] Dipartimento di Biologia Ambientale, Università di Roma "La Sapienza", Roma, Italy

[15] UMR 6249 Chrono-Environnement, Université de Franche-Comté, Besançon, France

Correspondence to: O. Peyron (odile.peyron@univ-montp2.fr)

28   Abstract

29   Climate evolution of the Mediterranean region during the Holocene exhibits strong spatial and

30   temporal variability. The spatial differentiation and temporal variability, as evident from

31   different climate proxy datasets, has remained notoriously difficult for models to reproduce. In

32   light of this complexity, we propose here a new paleo-observations synthesis and its comparison

33   – at regional/local level – with a climate model data to examine (i) opposing northern and

34   southern precipitation regimes during the Holocene across the Mediterranean basin, and (ii) an

35   east-to-west precipitation dipole during the early Holocene, from a wet eastern Mediterranean

36   to dry western Mediterranean. Using precipitation estimates inferred from marine and terrestrial

37   pollen archives, we focus on two key time intervals, the early to mid-Holocene (8000 to 6000

38   cal yrs BP) and the late Holocene (4000 to 2000 yrs BP), in order to test the above mentioned

39   hypotheses on a Mediterranean-wide scale, and we compare the results with model outputs from

40   a high-resolution regional climate model. Spatially, we focus on transects across the

41   Mediterranean basin from north to south and from west to east. Because seasonality represents

42   a key parameter in Mediterranean climates, special attention was given to the reconstruction of

43   season-specific climate information, notably summer and winter precipitation. The

44   reconstructed climatic trends corroborate a previously described north-south partition of

45   precipitation regimes during the Holocene, but more sites from the northern part of the

46   Mediterranean basin are needed to further substantiate these observations. During the early

47   Holocene, relatively wet conditions occurred in the south-central and eastern Mediterranean

48   region, while drier conditions prevailed from 45°N northwards. These patterns then appear to

49   reverse during the late Holocene, with similar to present day or slightly drier than present day

50   conditions in the south-central region. With regard to the existence of a west-east precipitation

51   dipole during the Holocene, our pollen-based climate data show that the strength of this dipole

52   is strongly linked to the seasonal parameter reconstructed; early Holocene summers show a

53   clear east-west division, with summer precipitation having been highest in Greece and the

54   eastern Mediterranean and lowest over the Italy and the western Mediterranean. Summer

55   precipitation in the east remained above modern values, even during the late Holocene interval.

56   In contrast, winter precipitation signals are less spatially coherent during the early Holocene

57   but low precipitation is evidenced during the late Holocene. A general drying trend occurred

58   from the early to the late Holocene, particularly in the central and eastern Mediterranean.

59   For the same time intervals, site-based pollen-inferred precipitation estimates were compared

60   with model outputs, more specifically with an existing database from a regional-scale

downscaling (HadRM3) of a set of global climate-model simulations (HadAM3). The high-resolution detail achieved through the downscaling is intended to enable a better comparison between 'site-based' paleo-reconstructions and gridded model data in the complex terrain of the Mediterranean; the climate model outputs and pollen-inferred precipitation estimates show some overall correspondence, though modeled changes are extremely small and at the absolute margins of statistical significance. There are suggestions that the eastern Mediterranean experienced wetter than present summer conditions during the early and late Holocene; the drying trend in winter from the early to the late Holocene also appears to be simulated. Although some simulated patterns are of marginal statistical significance at the large scale, the use of this high-resolution regional climate model highlights how the inherently "patchy" nature of climate signals and palaeo-records in the Mediterranean basin may lead to local signals much stronger than the large-scale pattern would suggest. Nevertheless, the east to west division in summer precipitation seems more marked in the pollen reconstruction than in the model outputs. The footprint of the anomalies (like today or dry winters, wet summers) has some similarities to modern analogue atmospheric circulation patterns associated with a strong westerly circulation in winter (positive AO/NAO) and a weak westerly circulation in summer associated with anti-cyclonic blocking; although there also remain important differences between the palaeo-simulations and these analogues. The regional climate model, consistent with other global models, does not suggest an extension of the African summer monsoon into the Mediterranean; so the extent to which summer monsoonal precipitation may have existed in the southern and eastern Mediterranean during the mid-Holocene remains an outstanding question.

1 Introduction

The Mediterranean region is particularly sensitive to climate change due to its position within the confluence of arid North African (i.e. subtropically influenced) and temperate/humid European (i.e. mid-latitudinal) climates (Lionello, 2012). Palaeoclimatic proxies, including stable isotopes, lipid biomarkers, palynological data and lake-levels, have shown that the Mediterranean region experienced climatic conditions that varied spatially and temporally throughout the Holocene (e.g. Bar-Matthews and Ayalon, 2011; Luterbacher et al., 2012; Lionello, 2012; Triantaphyllou et al., 2014, 2016; Mauri et al., 2015; De Santis and Caldara 2015; Sadori et al., 2016a) and well before (eg. Sadori et al., 2016b). Clear spatial climate patterns have been identified from east to west and from north to south within the basin (e.g. Zanchetta et al., 2007; Magny et al., 2009b, 2011, 2013; Zhornyak et al., 2011; Sadori et al., 2013; Fletcher et al., 2013). Lake-level reconstructions from Italy thus suggest contrasting patterns of palaeohydrological changes for the central Mediterranean during the Holocene (Magny et al., 2012, 2013). Specifically, lake level maxima occurred south of approximately 40ºN in the early to mid-Holocene, while lakes north of 40°N recorded minima. This pattern was reversed at around 4500 cal yrs BP (Magny et al., 2013). Quantitative pollen-based precipitation reconstructions from sites in northern Italy indicate humid winters and dry summers during the early to mid-Holocene, whereas southern Italy was characterised by humid winters and summers; the N-S pattern reverses in the late Holocene, with drier conditions at southern sites and wet conditions at northern sites (Peyron et al., 2011, 2013). These findings support a north–south partition for the central Mediterranean with regards to precipitation, and also confirm that precipitation seasonality is a key parameter in the evolution of Mediterranean climates. The pattern of shifting N-S precipitation regimes has also been identified for the Aegean Sea (Peyron et al., 2013). Taken together, the evidence from pollen data and from other proxies covering the Mediterranean region suggest a climate response that can be linked to a combination of orbital, ice-sheet and solar forcings (Magny et al., 2013).

An east-west pattern of climatic change during the Holocene is also suggested in the Mediterranean region (e.g. Combourieu Nebout et al., 1998; Geraga et al., 2010; Colmenero-Hildago et al., 2002; Kotthoff et al., 2008; Dormoy et al., 2009; Finne et al., 2011; Roberts et al., 2011, 2012; Luterbacher et al., 2012; Guiot and Kaniewski, 2015). An east-west division during the Holocene is observed from marine and terrestrial pollen records (Dormoy et al., 2009; Guiot and Kaniewski, 2015), lake-level reconstructions (Magny et al., 2013) and speleothem isotopes (Roberts et al. 2011).

This study aims to reconstruct and evaluate N-S and E-W precipitations patterns for the Mediterranean basin, over two key periods in the Holocene, the early Holocene 8000-6000 cal yrs BP, corresponding to the "Holocene climate optimum" and the late Holocene 4000-2000 cal yrs BP corresponding to a trend towards drier conditions. Precipitation reconstructions are particularly important for the Mediterranean region given that precipitation rather than temperature represents the dominant controlling factor on the Mediterranean environmental system during the early to mid-Holocene (Renssen et al., 2012). Moreover, the reconstruction of precipitation parameters seems robust for the Mediterranean area (Combourieu-Nebout et al., 2009; Mauri et al., 2015; Peyron et al., 2011, 2013; Magny et al., 2013).

Precipitation is estimated for five pollen records from Greece, Italy and Malta, and for eight marine pollen records along a longitudinal gradient from the Alboran Sea to the Aegean Sea. Because precipitation seasonality is a key parameter of change during the Holocene in the Mediterranean (Rohling et al., 2002; Peyron et al., 2011; Mauri et al., 2015), the quantitative climate estimates focus on reconstructing changes in summer and winter precipitation.

Paleoclimate proxy data are essential benchmarks for model intercomparison and validation (e.g. Morrill et al., 2012; Heiri et al., 2014). This holds particularly true considering that previous model-data intercomparisons have revealed substantial difficulties for GCMs in simulating key aspects of mid-Holocene climate (Hargreaves et al., 2013) for Europe (Mauri et al., 2014), and notably for southern Europe (Davis and Brewer, 2009; Mauri et al., 2015). We also aim to identify and quantify the spatio-temporal climate patterns in the Mediterranean basin for the two key intervals of the Holocene (8000–6000 and 4000–2000 cal yrs BP) based on regional-scale climate model simulations (Brayshaw et al., 2011a). Finally, we compare our pollen-inferred climate patterns with regional-scale climate model simulations in order to critically assess the consistency of the climate reconstructions revealed by these two complimentary routes.

The first originality of our approach is that we estimate the magnitude of precipitation changes and reconstruct climatic trends across the Mediterranean using both terrestrial and marine high-resolution pollen records. The signal reconstructed is then more regional than in the studies based on terrestrial records alone. Moreover, this study aims to reconstruct precipitations patterns for the Mediterranean basin over two key periods in the Holocene while the existing large-scale quantitative paleoclimate reconstructions for the Holocene are often limited to the mid-Holocene - 6000 yrs BP- (Cheddadi et al., 1997; Bartlein et al., 2011; Mauri et al., 2014), except the climate reconstruction for Europe proposed by the study of Mauri et al. (2015).

The second originality of our approach is that we propose a data/model comparison based on (1) two time-slices and not only the mid-Holocene, a standard benchmark time period for this kind of data–model comparison; (2) a high resolution regional model (RCM) which provides a better representation of local/regional processes and helps to better simulate the localized, "patchy", impacts of Holocene climate change, when compared to coarser global GCMs (e.g. Mauri et al., 2014); (3) changes in seasonality, particularly changes in summer atmospheric circulation which have not been widely investigated (Brayshaw et al., 2011).

2   Sites, pollen records, and models

The Mediterranean region is at the confluence of continental and tropical air masses. Specifically, the central and eastern Mediterranean is influenced by monsoonal systems, while the north-western Mediterranean is under stronger influence from mid-latitude climate regimes (Lionello et al., 2006). Mediterranean winter climates are strongly affected by storm systems originating over the Atlantic. In the western Mediterranean, precipitation is predominantly affected by the North Atlantic Oscillation (NAO), while several systems interact to control precipitation over the northern and eastern Mediterranean (Giorgi and Lionello, 2008). Mediterranean summer climates are dominated by descending high pressure systems that lead to dry/hot conditions, particularly over the southern Mediterranean where climate variability is strongly influenced by African and Asian monsoons (Alpert et al., 2006) with strong geopotential blocking anomalies over central Europe (Giorgi and Lionello, 2008; Trigo et al., 2006).

The palynological component of our study combines results from five terrestrial and eight marine pollen records to provide broad coverage of the Mediterranean basin (Fig. 1, Table 1). The terrestrial sequences comprise pollen records from lakes along a latitudinal gradient from northern Italy (Lakes Ledro and Accesa) to Sicily (Lake Pergusa), one pollen record from Malta (Burmarrad) and one pollen record from Greece (Tenaghi Philippon). The marine pollen sequences are situated along a longitudinal gradient across the Mediterranean Sea; from the Alboran Sea (ODP Site 976 and core MD95-2043), Siculo-Tunisian strait (core MD04-2797), Adriatic Sea (core MD90-917), and Aegean Sea (cores SL152, MNB-3, NS14, HCM2/22). For each record we used the chronologies as reported in the original publications (see Table 1 for references).

181 Climate reconstructions for summer and winter precipitation (Figs. 2 and 3) inferred from the

182 terrestrial sequences and marine pollen records were performed using the Modern Analogue

183 Technique (MAT; Guiot, 1990). The MAT compares fossil pollen assemblages to modern

184 pollen assemblages with known climate parameters. The MAT is calibrated using an expanded

185 surface pollen dataset with more than 3600 surface pollen samples from various European

186 ecosystems (Peyron et al., 2013). In this dataset, 2200 samples are from the Mediterranean

187 region, and the results shows that the analogues selected here are limited to the Mediterranean

188 basin. Since the MAT uses the distance structure of the data and essentially performs local

189 fitting of the climate parameter (as the mean of *n*-closest sites), it may be less susceptible to

190 increased noise in the data set, and less likely to report spurious values than others methods (for

191 more details on the method, see Peyron et al., 2011). *Pinus* is overrepresented in marine pollen

192 samples (Heusser and Balsam, 1977; Naughton et al., 2007), and as such *Pinus* pollen was

193 removed from the assemblages (both modern and fossil) for the calibration of marine records

194 using MAT. The reliability of quantitative climate reconstructions from marine pollen records

195 has been tested using marine core-top samples from the Mediterranean in Combourieu-Nebout

196 et al. (2009), which shows an adequate consistency between the present day observed and MAT

197 estimations for annual and summer precipitations values.

198 The climate model simulations used in the model-data comparison are taken from Brayshaw et

199 al. (2010, 2011a, 2011b). The HadAM3 global atmospheric model (resolution 2.5° latitude x

200 3.75° longitude, 19 vertical levels; Pope et al., 2000) is coupled to a slab ocean (Hewitt et al.,

201 2001) and used to perform a series of time slice experiments. Each time-slice simulation

202 corresponds to 20 model years after spin up (40 model years for pre-industrial). The time slices

203 correspond to "present-day" (1960-1990), 2000 cal BP, 4000 cal BP, 6000 cal BP and 8000 cal

204 BP conditions, and are forced with appropriate insolation (associated with changes in the

205 Earth's orbit), and atmospheric CO_2 and CH_4 concentrations. The heat fluxes in the ocean are

206 held fixed using values taken from a pre-industrial control run (i.e., the ocean 'circulation' is

207 assumed to be invariant over the time-slices) and there is no sea-level change, but sea-surface

208 temperatures are allowed to evolve freely. The coarse global output from the model for each

209 time slice is downscaled over the Mediterranean region using HadRM3 (i.e. a limited area

210 version of the same atmospheric model; resolution 0.44° x 0.44°, with 19 vertical levels). Unlike

211 the global model, HadRM3 is not coupled to an ocean model; instead, sea-surface temperatures

212 are derived directly from the HadSM3 output.

Following Brayshaw et al. (2011a), time slice experiments are grouped into "mid Holocene" (8000 BP and 6000 cal yrs BP) and "late Holocene" (4000 BP and 2000 cal yrs BP) experiments because (1) these two periods are sufficiently distant in the past to be substantially different from the present but close enough that the model boundary conditions are well known; (2) these two periods are rich in high resolution and well-dated palaeoecological sequences, providing a good spatial coverage suitable for large-scale model-data comparison. These two experiments aid interpretability and increase the signal-to-noise ratio (the change in forcing between adjacent time-slices is relatively small, making it difficult to detect). To aid comparison with proxies, changes in climate are expressed as differences with respect to the present day (roughly 1960-1990) rather than the pre-industrial control run: therefore the climate anomalies shown thus include a component which is attributable to anthropogenic increases in greenhouse gases in the industrial period, as well as longer term 'natural' changes (e.g., orbital forcing). We suggest it may be better to use 'present day' to be in closer agreement with the pollen data (modern samples) which use the late 20th century long-term averages (1961-1990). However, there are some quite substantial differences between model runs under 'present day' and 'preindustrial' forcings (Figure 4). Statistical significance is assessed with the Wilcoxon-Mann-Whitney significance test (Wilks, 1995).

The details of the climate model simulations are discussed at length in Brayshaw et al (2010, 2011a, 2011b). These includes a detailed discussion of verification under present climate, the model's physical/dynamical climate responses to Holocene period 'forcings', and comparison to other palaeoclimate modelling approaches (e.g., PMIP projects) and palaeo-climate syntheses. The GCM used (HadAM3 with a slab ocean) is comparable to the climate models in PMIP2, but a key advantages of the present dataset is: (a) the inclusion of multiple time-slices across the Holocene period; and (b) the additional high-resolution regional climate model downscaling enables the impact of local climatic effects within larger-scale patterns of change to be distinguished (e.g., the impact of complex topography or coastlines; see Brayshaw et al 2011a), potentially allowing clearer comparisons between site-based proxy-data and model output.

3   Results and Discussion

A North-South precipitation pattern?

245 Pollen evidence shows contrasting patterns of palaeohydrological changes in the central
246 Mediterranean. The early- to mid-Holocene was characterized by precipitation maxima south
247 of around 40°N while at the same time, northern Italy experienced precipitation minima; this
248 pattern reverses after 4500 cal yrs BP (Magny et al., 2012b; Peyron et al., 2013). Other proxies
249 suggest contrasting north-south hydrological patterns not only in central Mediterranean but also
250 across the Mediterranean (Magny et al., 2013), suggesting a more regional climate signal. We
251 focus here on two time periods (early to mid-Holocene and late Holocene), in order to test this
252 hypothesis across the Mediterranean, and to compare the results with regional climate
253 simulations for the same time periods.

254 Early to mid-Holocene (8000 to 6000 cal yrs BP)

255 Climatic patterns reconstructed from both marine and terrestrial pollen records seem to
256 corroborate the hypothesis of a north-south division in precipitation regimes during the
257 Holocene (Fig 2a). Our results confirm that northern Italy was characterized by drier conditions
258 (relative to modern) while the south-central Mediterranean experienced more annual, winter
259 and summer precipitation during the early to mid-Holocene (Fig. 2a). Only Burmarrad (Malta)
260 shows drier conditions in the early to mid-Holocene (Fig 2a), although summer precipitation
261 reconstructions are marginally higher than modern at the site. Wetter summer conditions in the
262 Aegean Sea suggest a regional, wetter, climate signal over the central and eastern
263 Mediterranean. Winter precipitation in the Aegean Sea is less spatially coherent than summer
264 signal, with dry conditions in the North Aegean Sea and or near-modern conditions in the
265 Southern Aegean Sea (Figs. 2a and 3).

266 Non-pollen proxies, including marine and terrestrial biomarkers (terrestrial n-alkanes), indicate
267 humid mid-Holocene conditions in the Aegean Sea (Triantaphyllou et al., 2014, 2016). Results
268 within the Aegean support the pollen-based reconstructions, but non-pollen proxy data are still
269 lacking at the basin scale in the Mediterranean, limiting our ability to undertake independent
270 evaluation of precipitation reconstructions.

271 Very few large-scale climate reconstruction of precipitation exist for the whole Holocene
272 (Bartlein et al., 2011; Mauri et al., 2014; Guiot and Kaniewski, 2015; Tarroso et al., 2016) and,
273 even at local scales, pollen-inferred reconstructions of seasonal precipitation are very rare (Wu
274 et al., 2007; Peyron et al., 2011, 2013; Combourieu-Nebout et al., 2013; Nourelbait et al., 2016).
275 Several studies focused on the 6000 cal years BP period; Wu et al. (2007) reconstruct regional
276 seasonal and annual precipitation and suggest that precipitation did not differ significantly from

modern conditions across the Mediterranean; however, scaling issues render it difficult to compare their results with the reconstructions presented here. Cheddadi et al. (1997) reconstruct wetter-than-modern conditions at 6000 yrs cal BP in southern Europe; however, their study uses only one record from Italy and measures the moisture availability index, which is not directly comparable to precipitation *sensu stricto*, since it integrates temperature and precipitation. At 6000 yrs cal BP, Bartlein et al. (2011) reconstruct Mediterranean precipitation at values between 100 and 500 mm higher than modern. Mauri et al. (2015), in an updated version of Davis et al. (2003), provide a quantitative climate reconstructions comparable to the seasonal precipitation reconstructions presented here. Compared to Davis et al. (2003), which focused on reconstruction of temperatures, Mauri et al. (2015) reconstructed seasonal precipitation for Europe and analyse their evolution throughout the Holocene. Mauri et al. (2015) results differ from the current study in using MAT with plant functional type scores and in producing gridded climate maps. Mauri et al. (2015) show wet summers in southern Europe (Greece and Italy) with a precipitation maximum between 8000 and 6000 cal yrs BP, where precipitation was ~20 mm/month higher than modern. As in our reconstruction, precipitation changes in the winter were small and not significantly different from present-day conditions. Our reconstructions are in agreement with Mauri et al. (2015), with similar to present day summer conditions above 45°N during the early Holocene and wetter than today summer conditions over much of the south-central Mediterranean south of 45°N, while winter conditions appear to be similar to modern values. Mauri et al. (2015) results inferred from terrestrial pollen records and the climatic trends reconstructed here from marine and terrestrial pollen records seem to corroborate the hypothesis of a north-south division in precipitation regimes during the early to mid-Holocene in central Mediterranean. However, more high-resolution above 45°N are still needed to validate this hypothesis.

Late Holocene (4000 to 2000 cal yrs BP)

Late Holocene reconstructions of winter and summer precipitation indicate that the pattern established during the early Holocene was reversed by 4000 cal yrs BP, with similar to present day or lower than present day precipitation in southern Italy, Malta and Siculo-Tunisian strait (Figs. 2b and 3). Annual precipitation reconstructions suggest drying relative to the early Holocene, with modern conditions in northern Italy, and modern conditions or drier than modern conditions in central and southern Italy during most of the late Holocene. Reconstructions for the Aegean Sea still indicate higher than modern summer and annual precipitation (Fig. 2b). Winter conditions reverse the early to mid-Holocene trend, with modern

310 conditions in the northern Aegean Sea and wetter than modern conditions in the southern

311 Aegean Sea (Fig. 3). Our reconstructions from all sites show a good fit with Mauri et al. (2015),

312 except for the Alboran Sea where we reconstruct relatively high annual precipitations, whereas

313 Mauri et al. (2015) reconstruct dry conditions, but here too, more sites are needed to confirm

314 or refute this pattern in Spain. Our reconstruction of summer precipitation for the eastern

315 Mediterranean is very similar to Mauri et al. (2015) where wet conditions are reported for

316 Greece and the Aegean Sea.

317

318 *An East-West precipitation pattern?*

319 A precipitation gradient, or an east-west division during the Holocene has been suggested for

320 the Mediterranean from pollen data and lakes isotopes (e.g. Dormoy et al., 2009; Roberts et al.,

321 2011; Guiot and Kaniewski, 2015). However, lake-levels and other hydrological proxies around

322 the Mediterranean Basin do not clearly support this hypothesis and rather show contrasting

323 hydrological patterns south and north of 40°N particularly during the Holocene climatic

324 optimum (Magny et al., 2013).

325 Early to mid-Holocene (8000 to 6000 cal yrs BP)

326 The pollen-inferred annual precipitation indicates unambiguously wetter than today conditions

327 south of 42°N in the western, central and eastern Mediterranean, except for Malta (Fig. 3). A

328 prominent feature of the summer precipitation signal is an east-west dipole with increasing

329 precipitation in the eastern Mediterranean (as for annual precipitation). In contrast, winter

330 conditions show less spatial coherence, although the western basin, Sicily and the Siculo-

331 Tunisian strait appear to have experienced higher precipitation than modern, while drier

332 conditions exist in the east and in north Italy (Fig. 2a).

333 Our reconstruction shows a good match to Guiot and Kaniewski (2015) who have also discussed

334 a possible east-to-west division in the Mediterranean with regard to precipitation (summer and

335 annual) during the Holocene. They report wet centennial-scale spells in the eastern

336 Mediterranean during the early Holocene (until 6000 years BP), with dry spells in the western

337 Mediterranean. Mid-Holocene reconstructions show continued wet conditions, with drying

338 through the late Holocene (Guiot and Kaniewski, 2015). This pattern indicates a see-saw effect

339 over the last 10,000 years, particularly during dry episodes in the Near and Middle East. Similar

340 to in our findings, Mauri et al. (2015) also reconstruct high annual precipitation values over

341 much of the southern Mediterranean, and a weak winter precipitation signal. Mauri et al. (2015)

342 confirm an east-west dipole for summer precipitation, with conditions drier or close to present

343 in south-western Europe and wetter in the central and eastern Mediterranean (Fig 2b). These
344 studies corroborate the hypothesis of an east-to-west division in precipitation during the early
345 to mid-Holocene in the Mediterranean as proposed by Roberts et al. (2011). Roberts et al.
346 (2011) suggest the eastern Mediterranean (mainly Turkey and more eastern regions)
347 experienced higher winter precipitation during the early Holocene, followed by an oscillatory
348 decline after 6000 yrs BP. Our findings reveal wetter annual and summer conditions in the
349 eastern Mediterranean, although the winter precipitation signal is less clear. However, the
350 highest precipitation values reported by Roberts et al. (2011) were from sites located in western-
351 central Turkey; these sites are absent in the current study. Climate variability in the eastern
352 Mediterranean during the last 6000 years is also documented in a number of studies based on
353 multiple proxies (Finné et al., 2011). Most palaeoclimate proxies indicate wet mid-Holocene
354 conditions (Bar-Matthews et al., 2003; Stevens et al., 2006; Eastwood et al., 2007; Kuhnt et al.,
355 2008; Verheyden et al., 2008) which agree well with our results; however most of these proxies
356 are not seasonally resolved.

357 Roberts et al. (2011) and Guiot and Kaniewski (2015) suggest that changes in precipitation in
358 the western Mediterranean were smaller in magnitude during the early Holocene, while the
359 largest increases occurred during the mid-Holocene, around 6000-3000 cal BP, before declining
360 to modern values. Speleothems from southern Iberia suggest a humid early Holocene (9000-
361 7300 cal BP) in southern Iberia, with equitable rainfall throughout the year (Walczak et al.,
362 2015) whereas our reconstructions for the Alboran Sea clearly show an amplified precipitation
363 seasonality (with higher annual/winter and similar to modern summer rainfall) for the Alboran
364 sites. It is likely that seasonal patterns defining the Mediterranean climate must have been even
365 stronger in the early Holocene to support the wider development of sclerophyll forests than
366 present in south Spain (Fletcher et al., 2013).

367 Late Holocene (4000 to 2000 cal yrs BP)

368 Annual precipitation reconstructions suggest drier or near-modern conditions in central Italy,
369 Adriatic Sea, Siculo-Tunisian strait and Malta (Figs. 2b and 3). In contrast, the Alboran and
370 Aegean Seas remain wetter. Winter and summer precipitation produce opposing patterns; a
371 clear east-west division still exists for summer precipitation, with a maximum in the eastern
372 and a minimum over the western and central Mediterranean (Fig. 2b). Winter precipitation
373 shows the opposite trend, with a minimum in the central Mediterranean (Sicily, Siculo-Tunisian
374 strait and Malta) and eastern Mediterranean, and a maximum in the western Mediterranean
375 (Figs. 2b and 3). Our results are also in agreement with lakes and speleothem isotope records

376   over the Mediterranean for the late Holocene (Roberts et al., 2011), and the Finné et al. (2011)
377   palaeoclimate synthesis for the eastern Mediterranean. There is a good overall correspondence
378   between trends and patterns in our reconstruction and that of Mauri et al. (2015), except for the
379   Alboran Sea. High-resolution speleothem data from southern Iberia show Mediterranean
380   climate conditions in southern Iberia between 4800 and 3000 cal BP (Walczak et al., 2015)
381   which is in agreement with our reconstruction. The Mediterranean climate conditions
382   reconstructed here for the Alboran Sea during the late Holocene is consistent with a climate
383   reconstruction available from the Middle Atlas (Morocco), which show a trend over the last
384   6000 years towards arid conditions as well as higher precipitation seasonality between 4000
385   and 2000 cal yrs BP (Nourelbait et al., 2016). There is also good evidence from many records
386   to support late Holocene aridification in southern Iberia. Paleoclimatic studies document a
387   progressive aridification trend since ~7000 cal yr BP (e.g. Carrion et al., 2010; Jimenez-Moreno
388   et al., 2015; Ramos-Roman et al., 2016), although a reconstruction of the annual precipitation
389   inferred from pollen data with the Probability Density Function method indicate stable and dry
390   conditions in the south of the Iberian Peninsula between 9000 and 3000 cal BP (Tarroso et al.,
391   2016).

392   The current study shows that a prominent feature of late Holocene climate is the east-west
393   division in summer precipitation: summers were overall dry or near-modern in the central and
394   western Mediterranean and clearly wetter in the eastern Mediterranean. In contrast, winters
395   were drier or near-modern in the central and eastern Mediterranean (Fig. 3) while they were
396   wetter only in the Alboran Sea.

397

398   *Data-model comparison*

399   Figure 3 shows the data-model comparisons for the early to mid-Holocene (a) and late Holocene
400   (b) compared to present values (in anomalies). Encouragingly, there is a good overall
401   correspondence between patterns and trends in pollen-inferred precipitation and model outputs.
402   Caution is required when interpreting climate model results, however, as many of the changes
403   depicted in Fig. 3 are very small and of marginal statistical significance, suggesting a high
404   degree of uncertainty around their robustness.

405   For the early to mid-Holocene, both model and data indicate wet annual and summer conditions
406   in Greece and in the eastern Mediterranean, and drier than today conditions in north Italy. There
407   are indications of an east to west division in summer precipitation simulated by the climate

model (e.g., between the ocean to the south of Italy and over Greece/Turkey), although the changes are extremely small with a level of significance of 70%. Furthermore, in the Aegean Sea, the model shows a good match with pollen-based reconstructions, suggesting that the increased spatial resolution of the regional climate model may help to simulate the localized, "patchy", impacts of Holocene climate change, when compared to coarser global GCMs (Fig. 3). In Italy, the model shows a good match with pollen-based reconstructions with regards to the contrasting north-south precipitation regimes, but there is little agreement between model output and climate reconstruction with regard to winter and annual precipitation in southern Italy. The climate model suggests wetter winter and annual conditions in the far western Mediterranean (i.e. France, western Iberia and the NW coast of Africa) – similar to pollen-based reconstructions – and near-modern summer conditions during summers (except in France and northern Africa). A prominent feature of winter precipitation simulated by the model and partly supported by the pollen estimates is the reduced early Holocene precipitation everywhere in the Mediterranean basin except in the south east.

Model and pollen-based reconstructions for the late Holocene indicate declining winter precipitation in the eastern Mediterranean and southern Italy (Sicily and Malta) relative to the early Holocene. In contrast, late Holocene summer precipitation is higher than today in Greece and in the eastern Mediterranean and near-modern in the central and western Mediterranean, and relatively lower than today in south Spain and north Africa. The east-west division in summer precipitation is strongest during the late Holocene in the proxy data and there are suggestions that it appears to be consistently simulated in the climate model; the signal is reasonably clear in the eastern Mediterranean (Greece and Turkey) but non-significant in central and western Mediterranean (Fig. 3).

Our findings can be compared with previous data-model comparisons based on the same set of climate model experiments; although here we take our reference period as 'present-day' (1960-1990) rather than preindustrial and thus include an additional 'signal' from recent anthropogenic greenhouse gas emissions. Previous comparisons nevertheless suggested that the winter precipitation signal was strongest in the northeastern Mediterranean (near Turkey) during the early Holocene and that there was a drying trend in the Mediterranean from the early Holocene to the late Holocene, particularly in the east (Brayshaw et al., 2011a; Roberts et al., 2011). This is coupled with a gradually weakening seasonal cycle of surface air temperatures towards the present.

It is clear that most global climate models (PMIP2, PMIP3) simulate only very small changes in summer precipitation in the Mediterranean during the Holocene (Braconnot et al., 2007a,b, 2012; Mauri et al., 2014). The lack of a summer precipitation signal is consistent with the failure of the northeastern extension of the West African monsoon to reach the southeastern Mediterranean, even in the early to-mid-Holocene (Brayshaw et al., 2011a). The regional climate model simulates a small change in precipitation compared to the proxy results, and it can be robustly identified as statistically significant. This is to some extent unsurprising, insofar as the regional climate simulations presented here are themselves "driven" by data derived from a coarse global model (which, like its PMIP2/3 peers, does not simulate an extension of the African monsoon into the Mediterranean during this time period). Therefore, questions remain about summer precipitation in the eastern Mediterranean during the Holocene. The underlying climate dynamics therefore need to be better understood in order to confidently reconcile proxy data (which suggest increased summer precipitation during the early Holocene in the Eastern Mediterranean) with climate model results (Mauri et al., 2014). Based on the high-resolution coupled climate model EC-Earth, Bosmans et al. (2015) show how the seasonality of Mediterranean precipitation should vary from minimum to maximum precession, indicating a reduction in precipitation seasonality, due to changes in storm tracks and local cyclogenesis (i.e. no direct monsoon required). Such high-resolution climate modeling studies (both global and regional) may prove a key ingredient in simulating the relevant atmospheric processes (both local and remote) and providing fine-grain spatial detail necessary to compare results to palaeo-proxy observations.

Another explanation proposed by Mauri et al. (2014) is linked to the changes in atmospheric circulation. Our reconstructed climate characterized by dry winters and wet summers shows a spatial pattern that is somewhat consistent with modern day variability in atmospheric circulation rather than simple direct radiative forcing by insolation. In particular, the gross NW-SE dipole of reconstructed winter precipitation anomalies is perhaps similar to that associated with a modern-day positive AO/NAO. The west coast of Spain is, however, also wetter in our early Holocene simulations which would seem to somewhat confound this simple picture of a shift to an NAO+ like state compared to present. In summer, an anti-cyclonic blocking close to Scandinavia may have caused a more meridional circulation, which brought dry conditions to northern Europe, but relatively cooler and somewhat wetter conditions to many parts of southern Europe. It is of note that some climate models which have been used for studying palaeoclimate have difficulty reproducing this aspect of modern climate (Mauri et al., 2014).

473 Future work based on transient Holocene model simulations are important, nevertheless,
474 transient-model simulations have also shown mid-Holocene data-model discrepancies (Fischer
475 and Jungclaus, 2011; Renssen et al., 2012). It is, however, suggested that further work is
476 required to fully understand changes in winter and summer circulation patterns over the
477 Mediterranean (Bosmans et al., 2015).

478

479 *Data limitations*

480 Classic ecological works for the Mediterranean (e.g. Ozenda 1975) highlight how precipitation
481 limits vegetation type in plains and lowland areas, but temperature gradients take primary
482 importance in mountain systems. Also, temperature and precipitation changes are not
483 independent, but interact through bioclimatic moisture availability and growing season length
484 (Prentice et al., 1996). This may be one reason why certain sites may diverge from model
485 outputs; the Alboran sites, for example, integrate pollen from the coastal plains through to
486 mountain (+1500m) elevations. At high elevations within the source area, temperature effects
487 become be more important than precipitation in determining the forest cover type. Therefore, it
488 is not possible to fully isolate precipitation signals from temperature changes. Particularly for
489 the semiarid areas of the Mediterranean, the reconstruction approach probably cannot
490 distinguish between a reduction in precipitation and an increase in temperature and PET, or vice
491 versa.

492 Along similar lines, while the concept of reconstructing winter and summer precipitation
493 separately is very attractive, it may be highlighting commenting on some limitations. Although
494 different levels of the severity or length of summer drought are an important ecological
495 limitation for vegetation, reconstructing absolute summer precipitation can be difficult because
496 the severity/length of bioclimatic drought is determined by both temperature and precipitation.
497 We are dealing with a season that has, by definition, small amounts of precipitation that drop
498 below the requirements for vegetation growth. Elevation is also of concern, as lowland systems
499 tend to be recharged by winter rainfall, but high mountain systems may receive a significant
500 part of precipitation as snowfall, which is not directly available to plant life. This may be
501 important in the long run for improving the interpretation of long-term Holocene changes and
502 contrasts between different proxies, such as lake-levels and speleothems. All of these points
503 may seem very picky on the ecology side, but they may have a real influence leading to
504 problems and mismatches between different proxies (e.g. Davis et al., 2003; Mauri et al., 2015).

Another important point is the question of human impact on the Mediterranean vegetation during the Holocene. Since human activity has influenced natural vegetation, distinguishing between vegetation change induced by humans and climatic change in the Mediterranean is a challenge requiring independent proxies and approaches. Therefore links and processes behind societal change and climate change in the Mediterranean region are increasingly being investigated (e.g. Holmgren et al., 2016; Gogou et al, 2016; Sadori et al., 2016a). Here, the behavior of the reconstructed climatic variables between 4000 and 2000 cal yrs BP is likely to be influenced by non-natural ecosystem changes due to human activities such as the forest degradation that began in lowlands, progressing to mountainous areas (Carrión et al., 2010). These human impacts add confounding effects for fossil pollen records and may lead to slightly biased temperature reconstructions during the late Holocene, likely biased towards warmer temperatures and lower precipitation. However, if human activities become more marked at 3000 cal yrs BP, they increase significantly over the last millennia (Sadori et al., 2016) which is not within the time scale studied here. Moreover there is strong agreement between summer precipitation and independently reconstructed lake-level curves (Magny et al., 2013). For the marine pollen cores, human influence is much more difficult to interpret given that the source area is so large, and that, in general, anthropic taxa are not found in marine pollen assemblages.

Conclusions

The Mediterranean is particularly sensitive to climate change but the extent of future change relative to changes during the Holocene remains uncertain. Here, we present a reconstruction of Holocene precipitation in the Mediterranean using an approach based on both terrestrial and marine pollen records, along with a model-data comparison based on a high resolution regional model. We investigate climatic trends across the Mediterranean during the Holocene to test the hypothesis of an alternating north-south precipitation regime, and/or an east-west precipitation dipole. We give particular emphasis to the reconstruction of seasonal precipitation considering the important role it plays in this system.

Climatic trends reconstructed in this study seem to corroborate the north-south division of precipitation regimes during the Holocene, with wet conditions in the south-central and eastern Mediterranean, and dry conditions above 45°N during the early Holocene, while the opposite pattern dominates during the late Holocene. This study also shows that a prominent feature of Holocene climate in the Mediterranean is the east-to-west division in precipitation, strongly linked to the seasonal parameter reconstructed. During the early Holocene, we observe an east-

to-west division with high summer precipitation in Greece and the eastern Mediterranean and a minimum over the Italy and the western Mediterranean. There was a drying trend in the Mediterranean from the early Holocene to the late Holocene, particularly in central and eastern regions but summers in the east remained wetter than today. In contrast, the signal for winter precipitation is less spatially consistent during the early Holocene, but it clearly shows similar to present day or drier conditions everywhere in the Mediterranean except in the western basin during the late Holocene.

The regional climate model outputs show a remarkable qualitative agreement with our pollen-based reconstructions, although it must be emphasised that the changes simulated are typically very small or of questionable statistical significance. Nevertheless, there are indications that the east to west division in summer precipitation reconstructed from the pollen records do appear to be simulated by the climate model. The model results also suggest that parts of the eastern Mediterranean experienced similar to present day or drier conditions in winter during the early and late Holocene and wetter conditions in annual and summer during the early and late Holocene (both consistent with the paleo-records).

Although this study has used regional climate model data, it must always be recalled that the regional model's high-resolution output is strongly constrained by a coarser-resolution global climate model, and the ability of global models to correctly reproduce large-scale patterns of change in the Mediterranean over the Holocene remains unclear (e.g. Mauri et al 2015). The generally positive comparison between model and data presented here may therefore simply be fortuitous and not necessarily replicated if the output from other global climate model simulations was downscaled in a similar way. However, it is noted that the use of higher-resolution regional climate models can offer significant advantages for data-model comparison insofar as they assist in resolving the inherently "patchy" nature of climate signals and palaeo-records. Notwithstanding the difficulties of correctly modeling large-scale climate change over the Holocene (with GCMs), we believe that regional downscaling may still be valuable in facilitating model-data comparison in regions/locations known to be strongly influenced by local effects (e.g., complex topography).

572

573 **Figure captions**

574 Figure 1: Locations of terrestrial and marine pollen records along a longitudinal gradient from
575   west to east and along a latitudinal gradient from northern Italy to Malta.
576   Ombrothermic diagrams are shown for each site, calculated with the NewLoclim
577   software program and database, which provides estimates of average climatic
578   conditions at locations for which no observations are available (ex.: marine pollen
579   cores).

580 Figure 2: Pollen-inferred climate estimates as performed with the Modern Analogues
581   Technique (MAT): annual precipitation, winter precipitation (winter = sum of
582   December, January and February precipitation) and summer precipitation (summer =
583   sum of June, July and August precipitation). Changes in climate are expressed as
584   differences with respect to the modern values (anomalies, mm/day). The modern
585   values are derived from the ombrothermic diagrams (cf Fig. 1). Two key intervals of
586   the Holocene corresponding to the two time slice experiments (Fig. 3) have been
587   chosen: 8000–6000 cal yrs BP (a) and 4000–2000 (b) cal yrs BP. The climate values
588   available during these periods have been averaged (stars).

589 Figure 3: Data-model comparison for mid and late Holocene precipitation, expressed in
590   anomaly compared to present-day (mm/day). Simulations are based on a regional
591   model (Brayshaw et al., 2010): standard model HadAM3 coupled to HadSM3
592   (dynamical model) and HadRM3 (high-resolution regional model. The hatched areas
593   indicate areas where the changes are not significant (70% rank-significance test).
594   Pollen-inferred climate estimates (stars) are the same as in Fig. 2: annual precipitation,
595   winter precipitation (winter = sum of December, January and February precipitation)
596   and summer precipitation (summer = sum of June, July and August precipitation).

597 Figure 4: Model simulation showing Present day minus Preindustrial precipitation anomalies
598   (hatching at 70%/statistical significance over the insignificant regions)

599 Table 1: Metadata for the terrestrial and marine pollen records evaluated.

600

References

Alpert, P., Baldi, M., Ilani, R., Krichak, S., Price, C., Rodó, X., Saaroni, H., Ziv, B., Kishcha, P., Barkan, J., Mariotti, A. and Xoplaki, E.: Relations between climate variability in the Mediterranean region and the Tropics: ENSO, South Asian and African monsoons, hurricanes and Saharan dust In: Lionello P, Malanotte-Rizzoli P, Boscolo R (eds) Mediterranean Climate Variability, Amsterdam, Elsevier 149-177, 2006.

Bar-Matthews, M., Ayalon, A., Gilmour, M., Matthews, A. and Hawkesworth, C.J.: Sea-land oxygen isotopic relationships from planktonic foraminifera and speleothems in the Eastern Mediterranean region and their implication for paleorainfall during interglacial intervals, Geochimica et Cosmochimica Acta 67, 3181-3199, 2003.

Bar-Matthews, M. and Ayalon, A.: Mid-Holocene climate variations revealed by high-resolution speleothem records from Soreq Cave, Israel and their correlations with cultural changes, Holocene, 21, 163–172, 2011.

Bartlein, P.J., Harrison, S.P., Brewer, S., Connor, S., Davis, B.A.S., Gajewski, K., Guiot, J., Harrison-Prentice, T.I., Henderson, A., Peyron, O., Prentice, I.C., Scholze, M., Seppä, H., Shuman, B., Sugita, S., Thompson, R.S., Viau, A.E, Williams, J., and Wu H.: Pollen-based continental climate reconstructions at 6 and 21 ka: a global synthesis, Climate Dynamics 37, 775-802, 2011.

Bosmans, J.H.C., Drijfhout, S.S., Tuenter, E., Hilgen, F.J., Lourens, L.J. and Rohling, E.J.: Precession and obliquity forcing of the freshwater budget over the Mediterranean, Quaternary Science Reviews, 123, 16-30, 2015.

Braconnot, P., Otto-Bliesner, B., Harrison, S., Joussaume, S., Peterchmitt, J.-Y., Abe-Ouchi, A., Crucifix, M., Driesschaert, E., Fichefet, Th., Hewitt, C. D., Kageyama, M., Kitoh, A., Laîné, A., Loutre, M.-F., Marti, O., Merkel, U., Ramstein, G., Valdes, P., Weber, S. L., Yu, Y., and Zhao, Y.: Results of PMIP2 coupled simulations of the Mid-Holocene and Last Glacial Maximum –Part 1: experiments and large-scale features, Clim. Past, 3, 261–277, 2007a.

Braconnot, P., Otto-Bliesner, B., Harrison, S., Joussaume, S., Peterchmitt, J.-Y., Abe-Ouchi, A., Crucifix, M., Driesschaert, E., Fichefet, Th., Hewitt, C. D., Kageyama, M., Kitoh, A., Loutre, M.-F., Marti, O., Merkel, U., Ramstein, G., Valdes, P., Weber, L., Yu, Y., and Zhao, Y.: Results of PMIP2 coupled simula-tions of the Mid-Holocene and Last Glacial Maximum

632 – Part 2: feedbacks with emphasis on the location of the ITCZ and mid- and high latitudes

633 heat budget, Clim. Past, 3, 279–296, 2007b.

634 Braconnot, P., Harrison, S., Kageyama, M., Bartlein, J., Masson, V., Abe-Ouchi, A., Otto-

635 Bliesner, B., and Zhao, Y.: Evaluation of climate models using palaeoclimatic data, Nat.

636 Clim. Change, 2, 417-424, 2012.

637 Brayshaw, D.J., Hoskins, B. and Black, E.: Some physical drivers of changes in the winter

638 storm tracks over the North Atlantic and Mediterranean during the Holocene. Philosophical

639 Transactions of the Royal Society A: Mathematical, Physical and Engineering Sciences, 368,

640 5185-5223, 2010.

641 Brayshaw, D.J., Rambeau, C.M.C., and Smith, S.J.: Changes in the Mediterranean climate

642 during the Holocene: insights from global and regional climate modelling, Holocene 21, 15-

643 31, 2011a.

644 Brayshaw, D.J., Black, E., Hoskins, B. and Slingo, J.: Past climates of the Middle East, In:

645 Mithen, S. and Black, E. (eds.) Water, Life and Civilisation: Climate, Environment and

646 Society in the Jordan Valley. International Hydrology Series. Cambridge University Press,

647 Cambridge, pp. 25-50, 2011b

648 Carrión, J.S., Fernández, S., Jiménez-Moreno, G., Fauquette, S., Gil-Romera, G., González-

649 Sampériz, P. and Finlayson, C.: The historical origins of aridity and vegetation degradation in

650 southeastern Spain, Journal of Arid Environments, 74, 731-736, 2010.

651 Cheddadi, R., Yu, G., Guiot, J., Harrison, S.P., and Prentice, I.C.: The climate of Europe 6000

652 years ago, Climate Dynamics 13, 1-9, 1997.

653 Colmenero-Hidalgo, E., Flores, J.-A., and Sierro, F.J. Biometry of Emiliania huxleyi and its

654 biostratigraphic significance in the eastern north Atlantic Ocean and Western Mediterranean

655 Sea in the last 20,000 years, Marine Micropaleontology, 46, 247-263, 2002.

656 Colombaroli, D., Vannière, B., Chapron, E., Magny, M., and Tinner, W. Fire–vegetation

657 interactions during the Mesolithic–Neolithic transition at Lago dell'Accesa, Tuscany, Italy,

658 The Holocene, 18, 679–692, 2008.

659 Combourieu-Nebout, N., Paterne, M., Turon, J.-L., and Siani, G.: A high-resolution record of

660 the Last Deglaciation in the Central Mediterranean Sea: palaeovegetation and

661 palaeohydrological evolution, Quaternary Sci. Rev., 17, 303–332, 1998.

662 Combourieu-Nebout, N., Londeix, L., Baudin, F., and Turon, J.L.: Quaternary marine and
663 continental palaeoenvironments in the Western Mediterranean Sea (Leg 161, Site 976,
664 Alboran Sea): Palynological evidences, Proceeding of the Ocean Drilling Project, scientific
665 results, 161, 457-468, 1999.

666 Combourieu-Nebout, N., Turon, J.L., Zahn, R., Capotondi, L, Londeix, L., and Pahnke, K.:
667 Enhanced aridity and atmospheric high pressure stability over the western Mediterranean
668 during North Atlantic cold events of the past 50 000 years, Geology, 30, 863-866, 2002.

669 Combourieu-Nebout, N., Peyron, O., Dormoy, I., Desprat, S., Beaudouin, C., Kotthoff, U.,
670 and Marret, F.: Rapid climatic variability in the west Mediterranean during the last 25 000
671 years from high resolution pollen data, Clim. Past, 5, 503-521, 2009.

672 Combourieu-Nebout, N., Peyron, O., Bout-Roumazeilles, V., Goring, S., Dormoy, I.,
673 Joannin, S., Sadori, L., Siani, G., and Magny, M.: Holocene vegetation and climate
674 changes in central Mediterranean inferred from a high-resolution marine pollen record
675 (Adriatic Sea), Clim. Past 9, 2023-2042, 2013.

676 Davis, B. A. S., Brewer, S., Stevenson, A. C., and Guiot, J.: The temperature of Europe
677 during the Holocene reconstructed from pollen data, Quaternary Sci. Rev., 22, 1701–1716,
678 2003.

679 Davis, B. A. S. and Brewer, S.: Orbital forcing and role of the latitudinal insolation/
680 temperature gradient, Clim. Dynam., 32, 143-165, 2009.

681 De Santis V. and Caldara M. The 5.5–4.5 kyr climatic transition as recorded by the
682 sedimentation pattern of coastal deposits of the Apulia region, southern Italy, Holocene, 2015

683 Desprat, S., Combourieu-Nebout, N., Essallami, L., Sicre, M. A., Dormoy, I., Peyron, O.,
684 Siani, G., Bout Roumazeilles, V., and Turon, J. L.: Deglacial and Holocene vegetation
685 and climatic changes in the southern Central Mediterranean from a direct land-sea
686 correlation, Clim. Past, 9, 767–787, 2013.

687 Djamali, M., Gambin, B., Marriner, N., Andrieu-Ponel, V., Gambin, T., Gandouin, E.,
688 Médail, F., Pavon, D., Ponel, P., and Morhange, C.: Vegetation dynamics during the early to
689 mid-Holocene transition in NW Malta, human impact versus climatic forcing, Vegetation
690 History and Archaeobotany 22, 367-380, 2013.

691 Dormoy, I., Peyron, O., Combourieu Nebout, N., Goring, S., Kotthoff, U., Magny, M, and
692 Pross, J.: Terrestrial climate variability and seasonality changes in the Mediterranean region

693 between 15,000 and 4,000 years B.P. deduced from marine pollen records, Clim. Past, 5, 615-
694 632, 2009.

695 Drescher-Schneider, R., de Beaulieu, J.L., Magny, M., Walter-Simonnet, A.V., Bossuet, G.,
696 Millet, L. Brugiapaglia, E., and Drescher A.: Vegetation history, climate and human impact
697 over the last 15 000 years at Lago dell'Accesa, Veg. Hist. Archaeobot., 16, 279–299, 2007.

698 Eastwood, WJ., Leng, M., Roberts, N. and Davis B.: Holocene climate change in the eastern
699 Mediterranean region: a comparison of stable isotope and pollen data from Lake Gölhisar,
700 southwest Turkey, J. Quaternary Science 22, 327–341, 2007.

701 Finné, M., Holmgren, K., Sundqvist, H.S., Weiberg, E., and Lindblom, M.: Climate in the
702 eastern Mediterranean, and adjacent regions, during the past 6000 years, J. Archaeol. Sci., 38,
703 3153-3173, 2011.

704 Fischer N., and Jungclaus, J. H.: Evolution of the seasonal temperature cycle in a transient
705 Holocene simulation: orbital forcing and sea-ice, Clim. Past, 7, 1139-1148, 2011.

706 Fletcher, W.J., and Sánchez Goñi, M.F.: Orbital- and sub-orbital-scale climate impacts on
707 vegetation of the western Mediterranean basin over the last 48,000 yr, Quat. Res. 70, 451-464,
708 2008.

709 Fletcher, W.J., Sanchez Goñi, M.F., Peyron, O., and Dormoy, I.: Abrupt climate changes of
710 the last deglaciation detected in a western Mediterranean forest record, Clim. Past 6, 245-264,
711 2010.

712 Fletcher, W.J., Debret, M., and Sanchez Goñi, M.F.: Mid-Holocene emergence of a low-
713 frequency millennial oscillation in western Mediterranean climate: Implications for past
714 dynamics of the North Atlantic atmospheric westerlies, The Holocene, 23, 153-166, 2013.

715 Gambin B., Andrieu-Ponel V., Médail F., Marriner N., Peyron O., Montade V., Gambin T.,
716 Morhange C., Belkacem D., and Djamali M.: 7300 years of vegetation history and
717 quantitative climate reconstruction for NW Malta: a Holocene perspective, Clim. Past 12,
718 273-297, 2016

719 Geraga, M., Ioakim, C., Lykousis, V., Tsaila-Monopolis, S., and Mylona, G.: The high-
720 resolution palaeoclimatic and palaeoceanographic history of the last 24,000 years in the
721 central Aegean Sea, Greece, Palaeogeogr. Palaeocl., 287, 101–115, 2010.

722 Giorgi, F. and Lionello, P.: Climate change projections for the Mediterranean region, Global
723 Planet. Change, 63, 90–104, 2008.

724 Gogou, A., Bouloubassi, I., Lykousis, V., Arnaboldi, M., Gaitani, P., and Meyers, P.A.:

725 Organic geochemical evidence of abrupt late glacial- Holocene climate changes in the North

726 Aegean Sea, Palaeogeogr. Palaeocl., 256, 1 – 20, 2007.

727 Gogou, A., Triantaphyllou, M., Xoplaki, E., Izdebski, A., Parinos, C., Dimiza, M.,

728 Bouloubassi, I., Luterbacher, J., Kouli, K., Martrat, B., Toreti, A., Fleitmann, D., Rousakis,

729 G., Kaberi, H., Athanasiou, M., and Lykousis, V.: Climate variability and socio-

730 environmental changes in the northern Aegean (NE Mediterranean) during the last 1500

731 years, Quaternary Science Reviews, 136, 209-228, 2016.

732 Guiot J.: Methodology of the last climatic cycle reconstruction in France from pollen data,

733 Palaeogeography, Palaeoclimatology, Palaeoecology, 80, 49–69, 1990.

734 Guiot, J. and Kaniewski, D.: The Mediterranean Basin and Southern Europe in a warmer

735 world: what can we learn from the past? Front. Earth Sci., 18, 2015.

736 Hargreaves, J.C., Annan, J.D., Ohgaito, R., Paul, A., and Abe-Ouchi, A.: Skill and reliability

737 of climate model ensembles at the Last Glacial Maximum and mid-Holocene, Clim. Past, 9,

738 811-823, 2013.

739 Heiri, O., Brooks, S.J., Renssen, H., and 26 authors: Validation of climate model-inferred

740 regional temperature change for late-glacial Europe, Nature Communications 5, 4914, 2014.

741 Heusser, L.E., and Balsam W.L.: Pollen distribution in the N.E. Pacific ocean, Quaternary

742 Research, 7, 45-62, 1977.

743 Hewitt, C.D., Senior, C.A., and Mitchell, J.F.B. :The impact of dynamic sea-ice on the

744 climatology and sensitivity of a GCM: A study of past, present and future climates, Climate

745 Dynamics 17: 655–668, 2001.

746 Holmgren, K., Gogou, A., Izdebski, A., Luterbacher, J., Sicre, M.A., and Xoplaki, A.:

747 Mediterranean Holocene Climate, Environment and Human Societies, Quaternary Science

748 Reviews, 136, 1-4, 2016.

749 Ioakim, Chr., Triantaphyllou, M., Tsaila-Monopolis, S., and Lykousis, V.: New

750 micropalaeontological records of Eastern Mediterranean marine sequences recovered offshore

751 of Crete, during HERMES cruise and their palaeoclimatic paleoceanographic significance.

752 Acta Naturalia de "L'Ateneo Parmense", 45(1/4): p. 152. In: Earth System Evolution and the

753 Mediterranean Area from 23 Ma to the Present", 2009.

754   Jimenez-Moreno, G., Rodriguez-Ramirez, A., Perez-Asensio, J.N., Carrion, J.S., Lopez-

755   Saez, J.A, Villarías-Robles J., Celestino-Perez, S., Cerrillo-Cuenca, E., Leon, A., and

756   Contreras, C.: Impact of late-Holocene aridification trend, climate variability and geodynamic

757   control on the environment from a coastal area in SW Spain, Holocene, 1-11, 2015

758   Joannin, S., Vannière, B., Galop, D., Peyron, O., Haas, J.N., Gilli, A., Chapron, E., Wirth, S.,

759   Anselmetti, F., Desmet, M., and Magny, M.: Climate and vegetation changes during the

760   Lateglacial and Early-Mid Holocene at Lake Ledro (southern Alps, Italy), Clim. Past 9, 913-

761   933, 2013.

762   Joannin, S., Brugiapaglia, E., de Beaulieu, J.L, Bernardo, L., Magny, M., Peyron, O., Goring,

763   S., and Vannière, B.: Pollen-based reconstruction of Holocene vegetation and climate in

764   southern Italy: the case of Lago Trifoglietti., Clim. Past, 8, 1973-1996, 2012.

765   Kotthoff, U., Pross, J., Müller, U.C., Peyron, O., Schmiedl, G., and Schulz, H. Climate

766   dynamics in the borderlands of the Aegean Sea during formation of Sapropel S1 deduced

767   from a marine pollen record, Quaternary Sci. Rev., 27, 832–845, 2008.

768   Kotthoff, U., Koutsodendris, A., Pross, J., Schmiedl, G., Bornemann, A., Kaul, C., Marino,

769   G., Peyron, O., and Schiebel, R. Impact of late glacial cold events on the Northern Aegean

770   region reconstructed from marine and terrestrial proxy data, J. Quat. Sci., 26, 86-96, 2011.

771   Kouli, K., Gogou, A., Bouloubassi, I., Triantaphyllou, M.V., Ioakim, Chr, Katsouras, G.,

772   Roussakis, G., and Lykousis, V.: Late postglacial paleoenvironmental change in the

773   northeastern Mediterranean region: Combined palynological and molecular biomarker

774   evidence, Quatern. Int., 261, 118-127, 2012.

775   Kuhnt, T., Schmiedl, G., Ehrmann, W., Hamann, Y., and Andersen, N.: Stable isotopic

776   composition of Holocene benthic foraminifers from the eastern Mediterranean Sea: past

777   changes in productivity and deep water oxygenation, Palaeogeography, Palaeoclimatology,

778   Palaeoecology 268, 106-115, 2008.

779   Lionello, P, Malanotte-Rizzoli, P, Boscolo, R, Alpert, P, Artale, V, Li, L., et al.: The

780   Mediterranean climate: An overview of the main characteristics and issues. In: Lionello P,

781   Malanotte-Rizzoli P and Boscolo R (eds) Mediterranean Climate Variability. Developments

782   in Earth & Environmental Sciences 4, Elsevier, 1–26, 2006.

783   Lionello, P. (Ed.): The climate of the Mediterranean region: From the past to the future,

784   Elsevier, ISBN: 9780124160422, 2012.

785 Luterbacher, J., García-Herrera, R., Akcer-On, S., Allan R., Alvarez-Castro M.C, and 41

786 authors: A review of 2000 years of paleoclimatic evidence in the Mediterranean. In: Lionello,

787 P. (Ed.), The Climate of the Mediterranean region: From the past to the future, Elsevier,

788 Amsterdam, The Netherlands, 2012.

789 Magny, M., de Beaulieu, J.L., Drescher-Schneider, R., Vannière, B., Walter-Simonnet, A.V.,

790 Miras, Y., Millet, L., Bossuet, G., Peyron, O., Brugiapaglia, E., and Leroux, A.: Holocene

791 climate changes in the central Mediterranean as recorded by lake-level fluctuations at Lake

792 Accesa (Tuscany, Italy), Quaternary Sci. Rev. 26, 1736–1758, 2007.

793 Magny, M., Vannière, B., Zanchetta, G., Fouache, E., Touchais, G., Petrika, L., Coussot, C.,

794 Walter-Simonnet, A.V., and Arnaud, F.: Possible complexity of the climatic event around

795 4300-3800 cal BP in the central and western Mediterranean, Holocene, 19, 823-833, 2009.

796 Magny, M., Vannière, B., Calo, C., Millet, L., Leroux, A., Peyron, O., Zanchetta, G., La

797 Mantia, T. and Tinner, W.: Holocene hydrological changes in south-western Mediterranean as

798 recorded by lake-level fluctuations at Lago Preola, a coastal lake in southern Sicily, Italy,

799 Quaternary Sci. Rev., 30, 2459-2475, 2011.

800 Magny, M., Joannin, S., Galop, D., Vannière, B., Haas, J.N, Bassetti, M., Bellintani, P.,

801 Scandolari, R., and Desmet, M.: Holocene palaeohydrological changes in the northern

802 Mediterranean borderlands as reflected by the lake-level record of Lake Ledro, northeastern

803 Italy, Quaternary Res., 77, 382-396, 2012a.

804 Magny, M., Peyron, O., Sadori, L., Ortu, E., Zanchetta, G., Vannière, B., and Tinner, W.:

805 Contrasting patterns of precipitation seasonality during the Holocene in the south- and north-

806 central Mediterranean, J. Quaternary Sci., 27, 290–296, 2012b.

807 Magny, M. and 29 authors: North-south palaeohydrological contrasts in the central

808 Mediterranean during the Holocene: tentative synthesis and working hypotheses, Clim. Past 9,

809 2043-2071, 2013.

810 Mauri, A., Davis, B., Collins, P.M. and Kaplan, J.: The climate of Europe during the

811 Holocene: A gridded pollen-based reconstruction and its multi-proxy evaluation, Quat. Sc.

812 Rev. 112, 109-127, 2014.

813 Mauri, A., Davis, B., Collins, P.M. and Kaplan, J.: The influence of atmospheric circulation

814 on the mid-Holocene climate of Europe: A data–model comparison, Clim. Past 10, 1925-

815 1938, 2015.

816   Morrill, C., Anderson, D.M, Bauer, B.A, Buckner, R.E., Gille, P., Gross, W.S., Hartman, M.,
817   and Shah, A.: Proxy benchmarks for intercomparison of 8.2 ka simulations, Clim. Past 9, 423-
818   432, 2013.

819   Naughton, F., Sanchez Goñi, M.F., Desprat, S., Turon, J.L., Duprat, J., Malaizé, B., Joli, C.,
820   Cortijo, E., Drago, T., and Freitas, M.C.: Present-day and past (last 25 000 years) marine
821   pollen signal off western Iberia, Marine Micropaleontology 62, 91-114, 2007.

822   Nourelbait, M., Rhoujjati, A., Benkaddour, A., Carré, M., Eynaud, F., Martinez, P. and
823   Cheddadi, R.: Climate change and ecosystems dynamics over the last 6000 years in the
824   Middle Atlas, Morocco, Clim. Past 12, 1029-1042, 2016.

825   Peyron, O., Goring, S., Dormoy, I., Kotthoff, U., Pross, J., de Bealieu, J.L., Drescher-
826   Schneider, R., and Magny, M.: Holocene seasonality changes in the central Mediterranean
827   region reconstructed from the pollen sequences of Lake Accesa (Italy) and Tenaghi Philippon
828   (Greece), Holocene, 21, 131-146, 2011.

829   Peyron, O., Magny, M., Goring, S., Joannin, S., de Beaulieu, J.-L., Brugiapaglia, E., Sadori,
830   L., Garfi, G., Kouli, K., Ioakim, C., and Combourieu-Nebout, N. Contrasting patterns of
831   climatic changes during the Holocene in the central Mediterranean (Italy) reconstructed from
832   pollen data, Clim. Past 9, 1233-2013, 2013.

833   Pope, V.D., Gallani, M.L., Rowntree, R.R. and Stratton, R.A.: The impact of new physical
834   parameterizations in the Hadley Centre climate model: HadAM3, Climate Dynamics, 16, 123-
835   146, 2000.

836   Pross, J., Kotthoff, U., Müller, U.C., Peyron, O., Dormoy, I., Schmiedl, G., Kalaitzidis, S.,
837   and Smith, A.M.: Massive perturbation in terrestrial ecosystems of the Eastern Mediterranean
838   region associated with the 8.2 kyr climatic event, Geology, 37, 887-890, 2009.

839   Pross, J., Koutsodendris, A., Christanis, K., Fischer, T., Fletcher, W.J., Hardiman, M.,
840   Kalaitzidis, S., Knipping, M., Kotthoff, U., Milner, A.M., Müller, U.C., Schmiedl, G.,
841   Siavalas, G., Tzedakis, P.C., and Wulf, S.: The 1.35-Ma-long terrestrial climate archive of
842   Tenaghi Philippon, northeastern Greece: Evolution, exploration and perspectives for future
843   research, Newsletters on Stratigraphy, 48, 253-276, 2015.

844   Ramos-Román, M.J., Jiménez-Moreno, G., Anderson, R.S., García-Alix, A., Toney, J.L.,
845   Jiménez-Espejo, F.J. and Carrión, J.S.: Centennial-scale vegetation and North Atlantic

846   Oscillation changes during the Late Holocene in the southern Iberia, Quaternary Science
847   Reviews, 143, 84-98, 2016.

848   Renssen, H., Seppa, H., Crosta, X., Goosse, H., and Roche, D.M.: Global characterization of
849   the Holocene Thermal Maximum, Quat. Sci. Rev., 48, 7-19, 2012.

850   Roberts, N., Brayshaw, D., Kuzucuoğlu, C., Perez, R., and Sadori, L.: The mid-Holocene
851   climatic transition in the Mediterranean: Causes and consequences, Holocene, 21, 3-13, 2011.

852   Roberts, N., Moreno, A., Valero-Garces, B. L., Corella, J. P., Jones, M., Allcock, S., et al.
853   Palaeolimnological evidence for an east-west climate see-saw in the mediterranean since AD
854   900, Glob. Planet. Change, 84-85, 23-34, 2012.

855   Rohling, E.J., Cane, T.R., Cooke, S., Sprovieri, M., Bouloubassi, I., Emeis, K.C. et al: African
856   monsoon variability during the previous interglacial maximum, Earth Planet. Sc. Lett., 202,
857   61-75, 2002.

858   Sadori, L. and Narcisi, B.: The postglacial record of environmental history from Lago di
859   Pergusa, Sicily, Holocene, 11, 655-671, 2001.

860   Sadori, L. and Giardini, M.: Charcoal analysis, a method to study vegetation and climate of
861   the Holocene: The case of Lago di Pergusa, Sicily (Italy), Geobios-Lyon, 40, 173-180, 2007.

862   Sadori, L., Zanchetta, G., and Giardini, M.: Last Glacial to Holocene palaeoenvironmental
863   evolution at Lago di Pergusa (Sicily, Southern Italy) as inferred by pollen, microcharcoal, and
864   stable isotopes, Quatern. Int., 181, 4-14, 2008.

865   Sadori, L., Jahns, S., and Peyron, O.: Mid-Holocene vegetation history of the central
866   Mediterranean, Holocene, 21, 117-129, 2011.

867   Sadori, L., Ortu, E., Peyron, O., Zanchetta, G., Vannière, B, Desmet, M., and Magny, M.: The
868   last 7 millennia of vegetation and climate changes at Lago di Pergusa (central Sicily, Italy),
869   Clim. Past, 9, 1969-1984, 2013.

870   Sadori, L., Giraudi, C. Masi, A., Magny, M., Ortu, E., Zanchetta, G., and Izdebski, A.
871   Climate, environment and society in southern Italy during the last 2000 years. A review of the
872   environmental, historical and archaeological evidence, Quaternary Science Reviews, 136,
873   173-188, 2016a.

874   Sadori, L., Koutsodendris, A., Masi, A., Bertini, A., Combourieu-Nebout, N., Francke, A.,
875   Kouli, K., Joannin, S., Mercuri, A.M, Panagiotopoulos, K., Peyron, O., Torri, P., Wagner, B.,

876 Zanchetta, G., and Donders, T.H.: Pollen-based paleoenvironmental and paleoclimatic

877 change at Lake Ohrid (SE Europe) during the past 500 ka, Biogeosciences, 12, 15461-15493,

878 2016b.

879 Schemmel, F., Niedermeyer, E.M., Schwab-Lavrič, V., Gleixner, G., Pross, J., and Mulch, A.:

880 Plant-wax dD values record changing Eastern Mediterranean atmospheric circulation patterns

881 during the 8.2 ka BP climatic event, Quaternary Science Reviews, 133, 96-107, 2016.

882 Stevens, L.R., Ito, E., Schwalb, A., and Wright, H.E.: Timing of atmospheric precipitation in

883 the Zagros Mountains inferred from a multi-proxy record from Lake Mirabad, Iran, Quat.

884 Res. 66, 494-500, 2006.

885 Tarroso, P., Carrión, J., Dorado-Valiño, M., Queiroz, P., Santos, L., Valdeolmillos-Rodríguez,

886 A., Célio Alves, P., Brito, J. C., and Cheddadi, R.: Spatial climate dynamics in the Iberian

887 Peninsula since 15 000 yr BP, Clim. Past, 12, 1137-1149, 2016.

888 Triantaphyllou, V., Antonarakou, A., Kouli, K., Dimiza, M., Kontakiotis, G., Papanikolaou,

889 M.D. et al.: Late Glacial–Holocene ecostratigraphy of the south-eastern Aegean Sea, based on

890 plankton and pollen assemblages, Geo-Mar. Lett., 29, 249-267, 2009a.

891 Triantaphyllou, M.V., Ziveri, P., Gogou, A., Marino, G., Lykousis, V., Bouloubassi, I.,

892 Emeis, K.-C., Kouli, K., Dimiza, M., Rosell-Mele, A., Papanikolaou, M., Katsouras, G., and

893 Nunez, N.: Late Glacial-Holocene climate variability at the south-eastern margin of the

894 Aegean Sea, Mar. Geol., 266, 182-197, 2009b.

895 Triantaphyllou, M.V., Gogou, A, Bouloubassi, I., Dimiza, M, Kouli, K., Rousakis, A.G.,

896 Kotthoff, U., Emeis, K.C., Papanikolaou, M., Athanasiou, M., Parinos, C., Ioakim, C., V. and

897 Lykousis, V.: Evidence for a warm and humid Mid-Holocene episode in the Aegean and

898 northern Levantine Seas (Greece, NE Mediterranean), Regional Environmental Change, 14,

899 1697-1712, 2014.

900 Triantaphyllou, M.V., Gogou, A., Dimiza, M.D., Kostopoulou, S., Parinos, C., Roussakis, G.,

901 Geraga, M., Bouloubassi, I., Fleitmann, D., Zervakis, V., Velaoras, D., Diamantopoulou, A.,

902 Sampataki, A. and Lykousis, V.: Holocene Climate Optimum centennial-scale

903 paleoceanography in the NE Aegean Sea (Mediterranean Sea), Geo-Marine Letters, 36, 51-66,

904 2016.

905 Trigo R.M. and 21 coauthors: Relations between variability in the Mediterranean region and

906 Mid-latitude variability. In: Lionello P, Malanotte-Rizzoli P., Boscolo R., Eds., The

907   Mediterranean Climate: An overview of the main characteristics and issues. Elsevier,

908   Amsterdam, 2006.

909   Tzedakis, P.C.: Seven ambiguities in the Mediterranean palaeoenvironmental narrative,

910   Quaternary Sci. Rev., 26, 2042-2066, 2007.

911   Vannière, B., Power, M.J., Roberts, N., Tinner, W., Carrion, J., Magny, M., Bartlein, P., and

912   Contributors Data: Circum-Mediterranean fire activity and climate changes during the mid

913   Holocene environmental transition (8500-2500 cal yr BP), Holocene, 21, 53-73, 2011.

914   Vannière, B., Magny, M. , Joannin, S. , Simonneau, A. , Wirth, S.B. , Hamann, Y., Chapron,

915   E., Gilli, A., Desmet, M., and Anselmetti, F.S.: Orbital changes, variation in solar activity and

916   increased anthropogenic activities: controls on the Holocene flood frequency in the Lake

917   Ledro area, Northern Italy, Clim. Past, 9, 1193-1209, 2013.

918   Verheyden S., Nader F.H., Cheng H.J., Edwards L.R. and Swennen R.: Paleoclimate

919   reconstruction in the Levant region from the geochemistry of a Holocene stalagmite from the

920   Jeita cave, Lebanon, Quaternary Research, 70, 368-381, 2008.

921   Walczak, I.W., Baldini, J.U.L., Baldini, L.M., Mcdermott, F., Marsden, S., Standish, C.D,

922   Richards, D.A., Andreo, B and Slater J.: Reconstructing high-resolution climate using CT

923   scanning of unsectioned stalagmites: A case study identifying the mid-Holocene onset of the

924   Mediterranean climate in southern Iberia, Quaternary Science Reviews 127, 117-128, 2015.

925   Wilks D. S.: Statistical methods in the atmospheric sciences (Academic Press, San Diego,

926   CA), 1995.

927   Wood, S.N. Fast stable restricted maximum likelihood and marginal likelihood estimation of

928   semiparametric generalized linear models. Journal of the Royal Statistical Society (B) 73(1),

929   3-36, 2011.

930   Wu, H., Guiot, J., Brewer, S., and Guo, Z.: Climatic changes in Eurasia and Africa

931   at the Last Glacial Maximum and mid-Holocene: reconstruction from pollen data using

932   inverse vegetation modelling, Clim. Dyn., 29, 211-229, 2007.

933   Zanchetta, G., Borghini, A., Fallick, A.E., Bonadonna, F.P., and Leone, G.: Late Quaternary

934   palaeohydrology of Lake Pergusa (Sicily, southern Italy) as inferred by stable isotopes of

935   lacustrine carbonates, J. Paleolimnol., 38, 227-239, 2007.

936   Zhornyak, L.V., Zanchetta, G., Drysdale, R.N., Hellstrom, J.C., Isola, I., Regattieri, E.,

937   Piccini, L., Baneschi, I., and Couchoud, I.: Stratigraphic evidence for a "pluvial phase"

938   between ca. 8200-7100 ka from Renella cave (Central Italy), Quat. Sci. Rev., 30, 409-417,

939   2011.
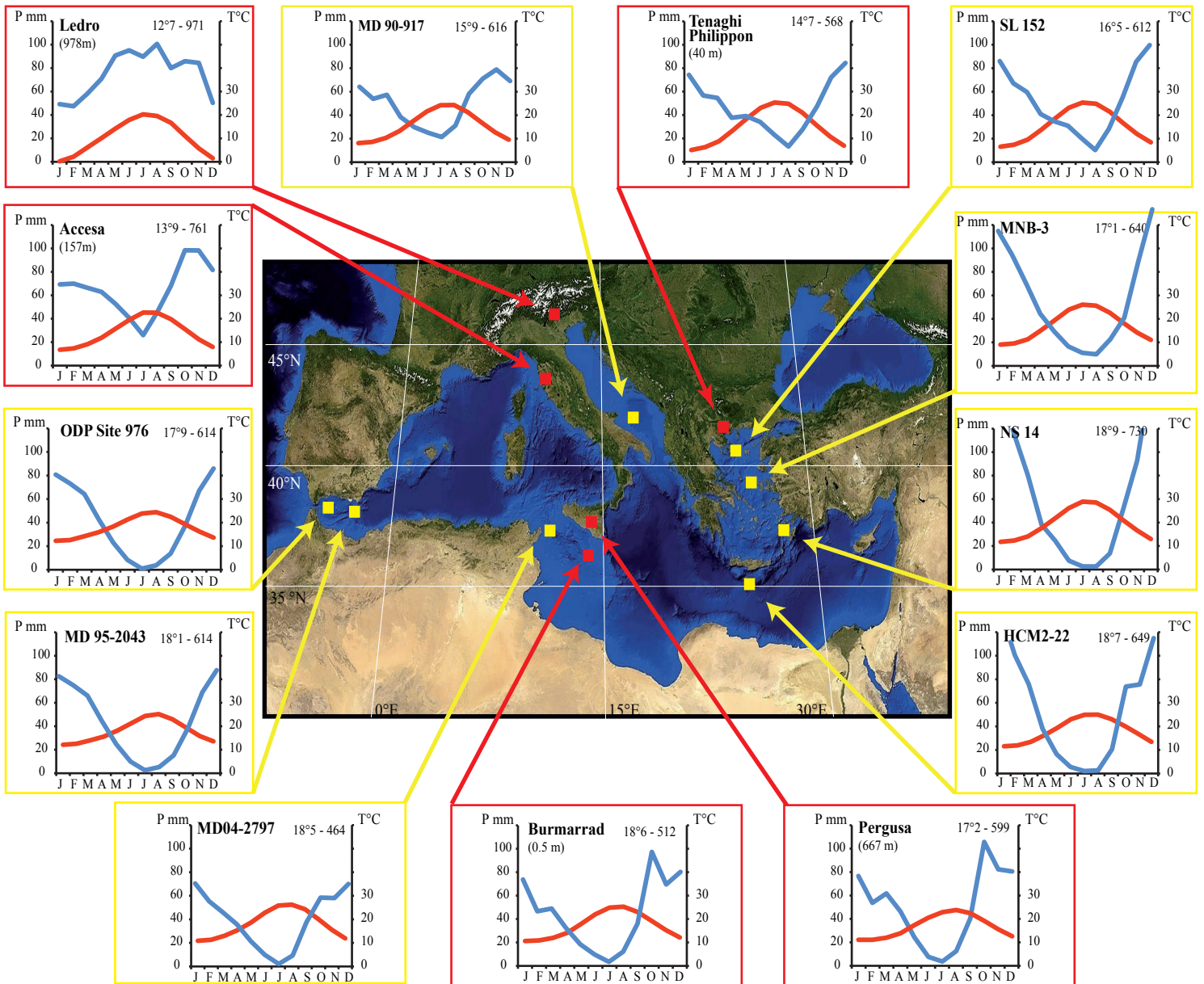
Figure 1: Locations of terrestrial (red) and marine (yellow) pollen records.
Ombrothermic diagrams are calculated with the NewLoclim software, which provides estimates of average climatic conditions at locations for which no observations are available (ex.: marine pollen cores).

Annual precipitation 8000-6000 cal yrs BP
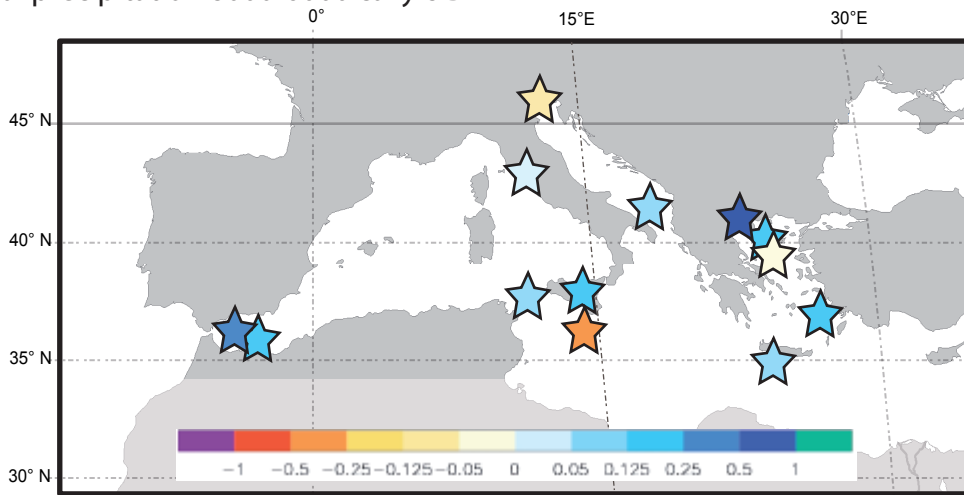
Winter precipitation 8000-6000 cal yrs BP
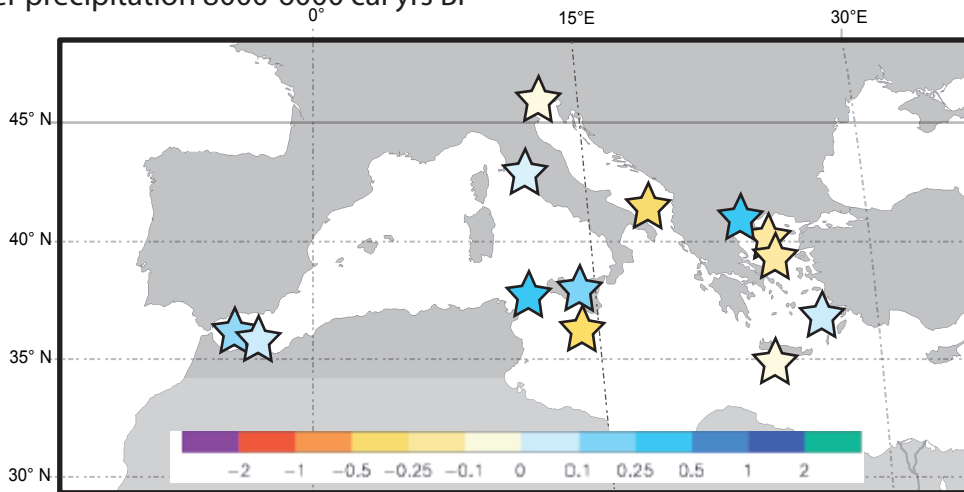

Summer precipitation 8000-6000 cal yrs BP
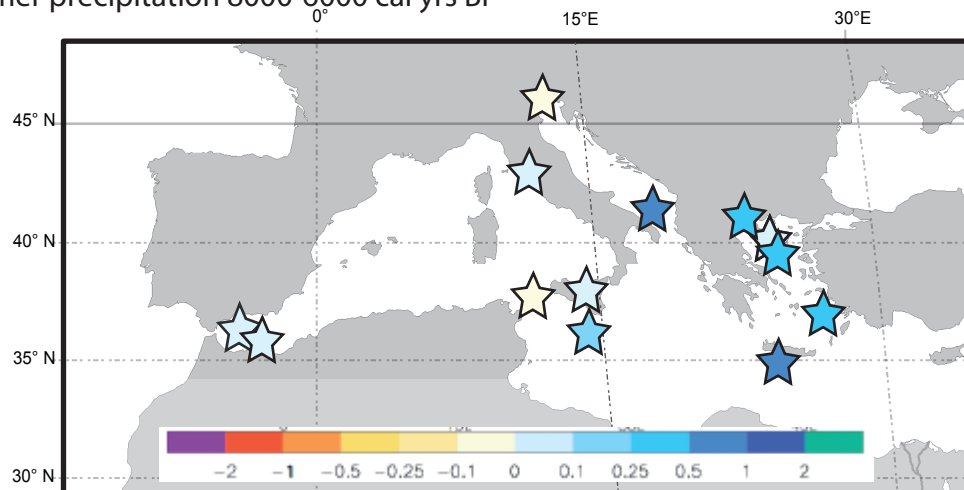
Figure 2a: 8000-6000 cal years BP
 Pollen-inferred climate estimates as performed with the Modern Analogues Technique: annual precipitation, winter precipitation (winter = sum of December, January and February precipitation) and summer precipitation (summer = sum of June, July and August precipitation). Changes in climate are expressed as differences with respect to the modern values (anomalies, mm/day), which are derived from the ombrothermic diagrams (cf Fig. 1). Climate values reconstructed during the 8000-6000 cal yrs BP have been averaged (stars).

Annual precipitation 4000-2000 cal yrs BP
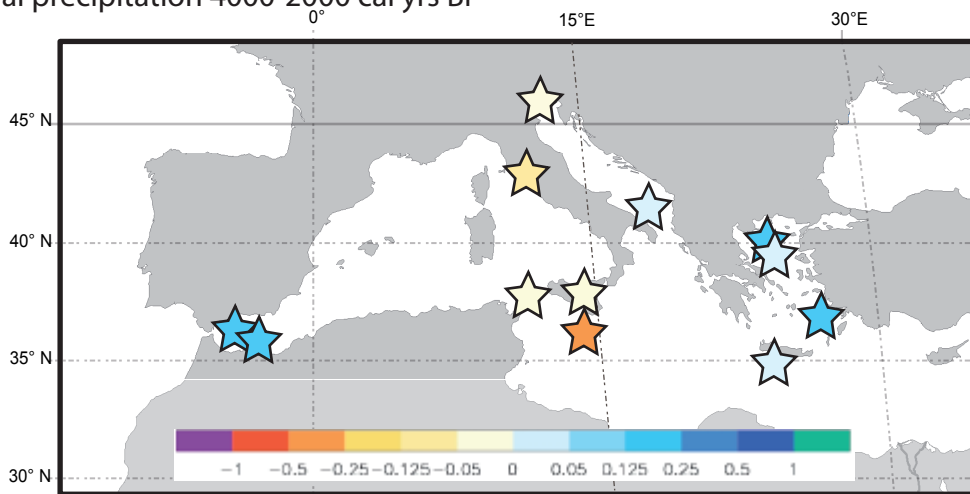
Winter precipitation 4000-2000 cal yrs BP
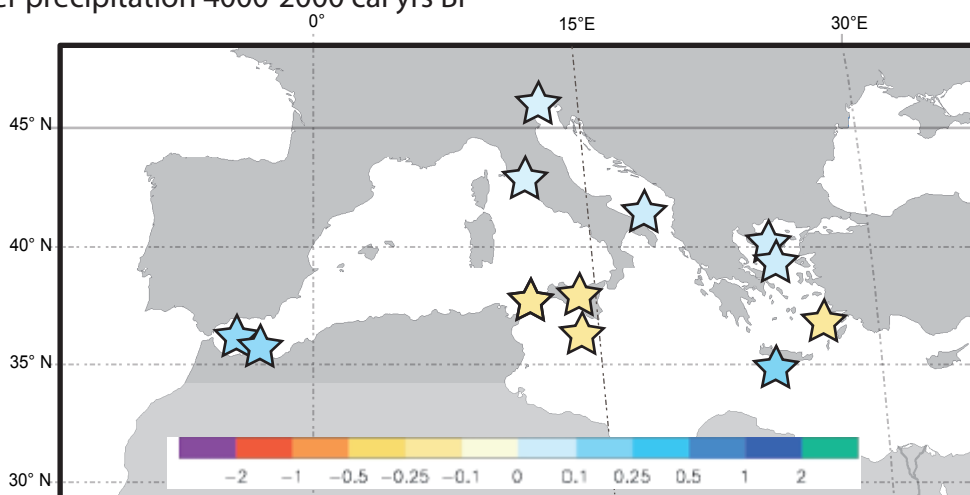
## Summer precipitation 4000-2000 cal yrs BP
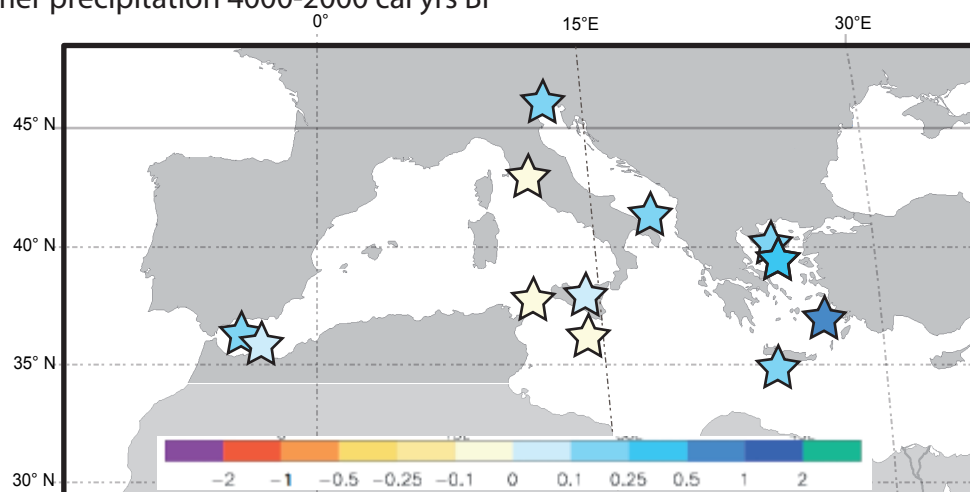
Figure 2b: 4000-2000 cal yrs BP

Pollen-inferred climate estimates as performed with the Modern Analogues Technique: annual precipitation, winter precipitation (winter = sum of December, January and February precipitation) and summer precipitation (summer = sum of June, July and August precipitation). Changes in climate are expressed as differences with respect to the modern values (anomalies, mm/day), which are derived from the ombrothermic diagrams (cf Fig. 1). Climate values reconstructed during the 4000-2000 cal yrs BP have been averaged (stars).
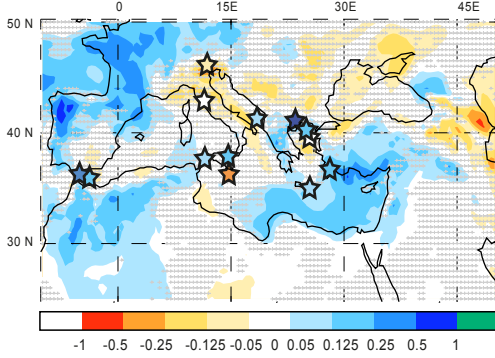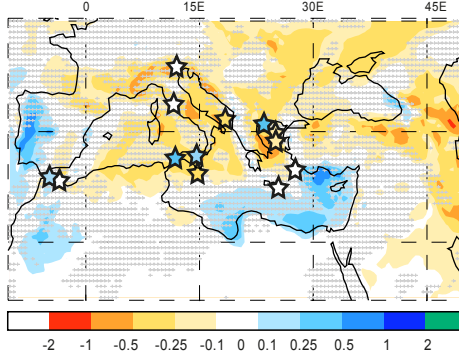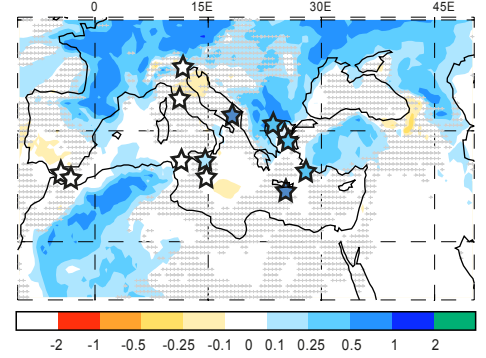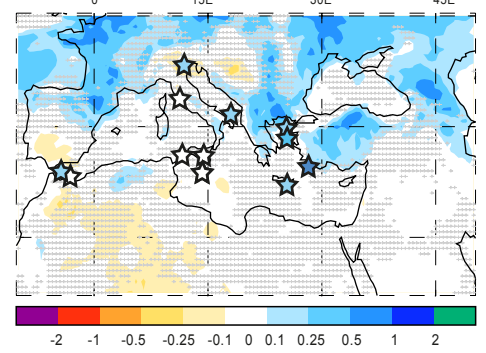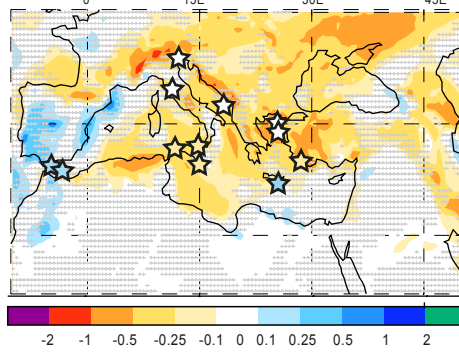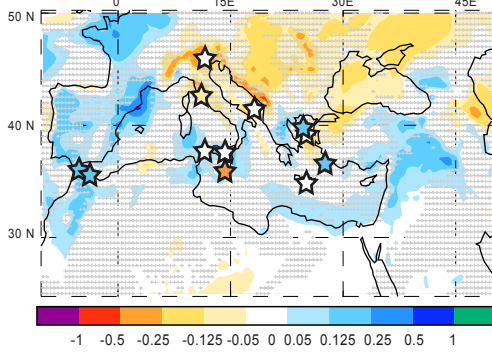
Figure 3: Data-model comparison for mid and late Holocene precipitation, expressed in anomaly (mm/day)
Simulations are based on a regional model (Brayshaw et al., 2010): standard model HadAM3 coupled to HadSM3
and HadRM3 (high-resolution regional model). The hatched areas indicate areas where the changes are not significant (threshold used here 70%).
Pollen-inferred climate estimates (stars) are the same as in Fig.2: annual precipitation, winter precipitation and summer precipitation .
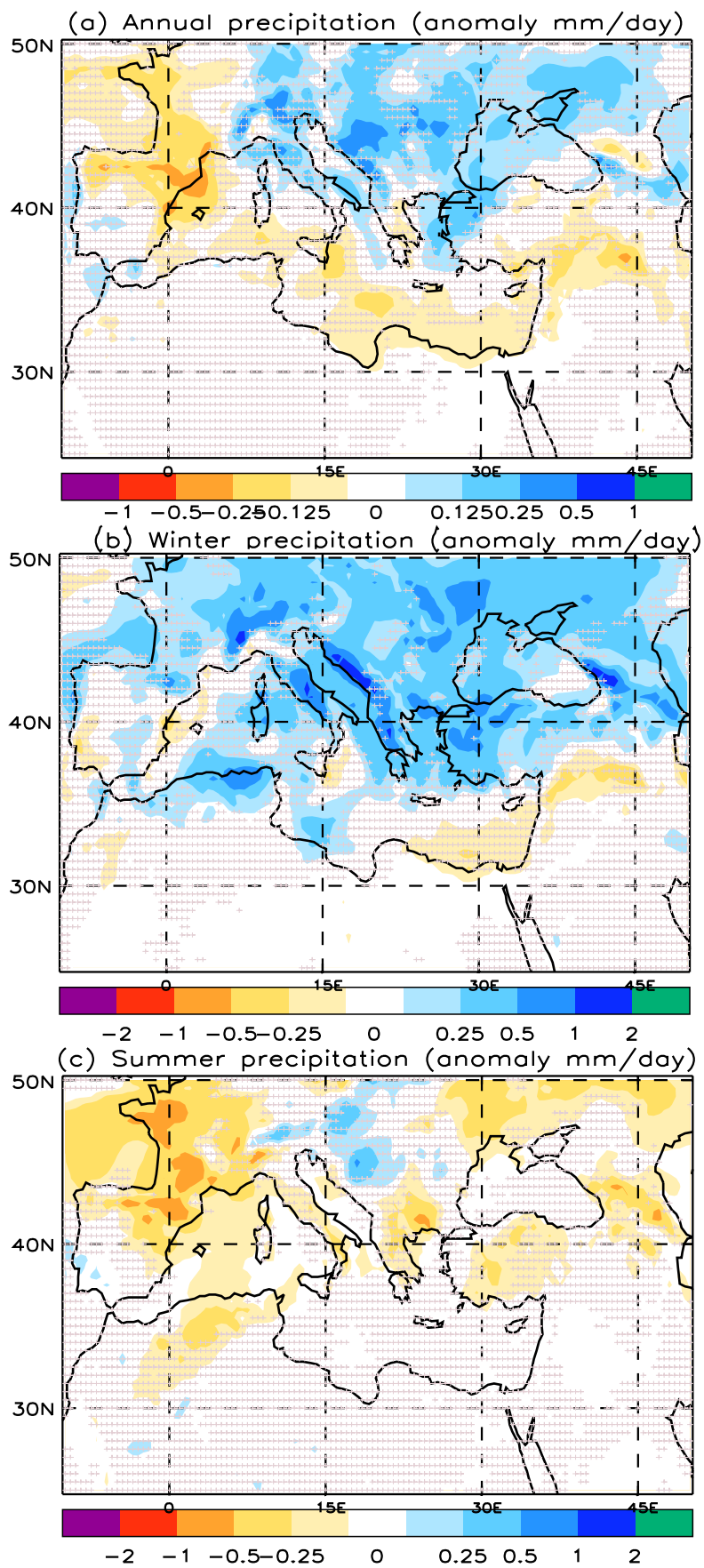
Figure 4: Model simulation showing Present day minus Preindustrial precipitation anomalies
(hatching at 70%/statistical significance over the insignificant regions)

Terrestrial pollen records

	Longit.	Latitude	Elev. (m a.s.l)	Temporal resolution	References (non- exhaustive)
Ledro (North Italy)	10°76'E	45°87'N	652	8000-6000: 71 4000-2000: 60 10966-10: 66	Joannin et al. (2013), Magny et al. (2009, 2012a), Vannière et al. (2013), Peyron et al. (2013)
Accesa (Central Italy)	10°53'E	42°59'N	157	8000-6000: 90 4000-2000 : 133 11029-100: 97	Drescher-Schneider et al. (2007), Magny et al. (2007, 2013), Colombaroli et al. (2008), Sadori et al. (2011), Vannière et al. (2011), Peyron et al. (2011, 2013)
Trifoglietti (Southern Italy)	16°01'E	39°33'N	1048	8000-6000: 95 4000-2000: 86 9967-14: 73	Joannin et al. (2012), Peyron et al. (2013)
Pergusa (Sicily)	14°18'E	37°31'N	667	8000-6000: 166 4000-2000: 90 12749-53: 154	Sadori and Narcisi (2001); Sadori et al. (2008, 2011, 2013, 2016b); Magny et al. (2011, 2013)
Tenaghi Philippon (Greece)	24°13.4'E	40°58.4'N	40	8000-6000: 64 4000-2000: no 10369-6371:53	Pross et al. (2009, 2015), Peyron et al. (2011), Schemmel et al., (2016)
Burmarrad (Malta)	14°25'E	35°56'N	0.5	8000-6000: 400 4000-2000: 285 6904-1730: 110	Djamali et al. (2013), Gambin et al., (2016)

Marine pollen records

	Longit.	Latitude	Water-depth	Temporal resolution	References
ODP 976 (Alboran Sea)	4°18'W	36°12' N	1108	8000-6000: 142 4000-2000: 181 10903-132: 129	Combourieu-Nebout et al. (1999, 2002, 2009) ; Dormoy et al., (2009)
MD95-2043 (Alboran Sea)	2°37'W	36°9'N	1841	8000-6000: 111 4000-2000: 142 10952-1279: 106	Fletcher and Sánchez Goñi (2008); Fletcher et al., (2010)
MD90-917 (Adriatic Sea)	17°37'E	41°97'N	845	8000-6000: 90 4000-2000: 333 10495-2641: 122	Combourieu-Nebout et al. (2013)
MD04-2797 (Siculo-Tunisian strait)	11°40'E	36°57'N	771	8000-6000: 111 4000-2000: 666 10985-2215: 127	Desprat et al. (2013)
SL152 (North Aegean Sea)	24°36' E	40°19' N	978	8000-6000: 60 4000-2000: 95 9999-0: 76	Kotthoff et al. (2008, 2011), Dormoy et al. (2009).
NS14 (South Aegean Sea)	27°02'E	36°38'N	505	8000-6000: 80 4000-2000: 333 9988-2570: 107	Kouli et al. (2012) ; Gogou et al. (2007); Triantaphyllou et al. (2009a, b)
HCM2/22 (South Crete)	24°53'E	34°34 N	2211	8000-6000: 181 4000-2000: 333 8091-2390: 247	Ioakim et.al. (2009) ; Kouli et al, (2012) ; Triantaphyllou et al. (2014)

MNB-3 (North Aegean Sea)	25°00'E	39°15'N	800	8000-6000: 153	Geraga et al. (2010) ; Kouli et al.,
				4000-2000: 166	(2012) ; Triantaphyllou et al,
				8209-2273: 138	(2014)

Table 1: Metadata for the terrestrial and marine pollen records evaluated. The temporal resolution is calculated for the two periods (8000-6000 and 4000-2000) and for the entire record.